

This is a self-archived version of an original article. This version may differ from the original in pagination and typographic details.

Author(s): Nesterenko, Dmitrii; Canete, Laetitia; Eronen, Tommi; Jokinen, Ari; Kankainen, Anu; Novikov, Yu.N.; Rinta-Antila, Sami; de Roubin, Antoine; Vilén, Markus

Title: High-precision measurement of the mass difference between ^{102}Pd and ^{102}Ru

Year: 2019

Version: Accepted version (Final draft)

Copyright: © 2018 Elsevier B.V.

Rights: CC BY-NC-ND 4.0

Rights url: <https://creativecommons.org/licenses/by-nc-nd/4.0/>

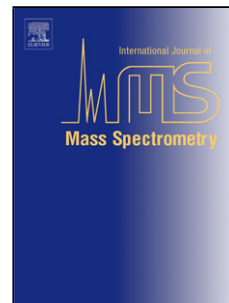
Please cite the original version:

Nesterenko, D., Canete, L., Eronen, T., Jokinen, A., Kankainen, A., Novikov, Yu.N., Rinta-Antila, S., de Roubin, A., & Vilén, M. (2019). High-precision measurement of the mass difference between ^{102}Pd and ^{102}Ru . *International Journal of Mass Spectrometry*, 435, 204-208.
<https://doi.org/10.1016/j.ijms.2018.10.038>

Accepted Manuscript

Title: High-precision measurement of the mass difference between ^{102}Pd and ^{102}Ru

Author: D.A. Nesterenko L. Canete T. Eronen A. Jokinen A. Kankainen Yu.N. Novikov S. Rinta-Antila A. de Roubin M. Vilen



PII: S1387-3806(18)30325-7
DOI: <https://doi.org/doi:10.1016/j.ijms.2018.10.038>
Reference: MASPEC 16073

To appear in: *International Journal of Mass Spectrometry*

Received date: 20 August 2018
Revised date: 22 October 2018
Accepted date: 29 October 2018

Please cite this article as: D.A. Nesterenko, L. Canete, T. Eronen, A. Jokinen, A. Kankainen, Yu.N. Novikov, S. Rinta-Antila, A. de Roubin, M. Vilen, High-precision measurement of the mass difference between ^{102}Pd and ^{102}Ru , *International Journal of Mass Spectrometry* (2018), <https://doi.org/10.1016/j.ijms.2018.10.038>

This is a PDF file of an unedited manuscript that has been accepted for publication. As a service to our customers we are providing this early version of the manuscript. The manuscript will undergo copyediting, typesetting, and review of the resulting proof before it is published in its final form. Please note that during the production process errors may be discovered which could affect the content, and all legal disclaimers that apply to the journal pertain.

High-precision measurement of the mass difference between ^{102}Pd and ^{102}Ru D.A. Nesterenko^{a,b,*}, L. Canete^a, T. Eronen^a, A. Jokinen^a, A. Kankainen^a, Yu.N. Novikov^{b,c}, S. Rinta-Antila^a,
A. de Roubin^a, M. Vilen^a^aUniversity of Jyväskylä, P.O. Box 35, FI-40014 University of Jyväskylä, Finland^bPetersburg Nuclear Physics Institute, Gatchina 188300, Leningrad region, Russia^cSt. Petersburg State University, 7/9 Universitetskaya nab., St. Petersburg 199034, Russia**Abstract**

The Q -value for the neutrinoless double electron capture on ^{102}Pd , $Q_{\text{ee}}(^{102}\text{Pd})$, is determined as the atomic mass difference between ^{102}Pd and ^{102}Ru . A precise measurement of the $Q_{\text{ee}}(^{102}\text{Pd})$ at the SHIPTRAP Penning trap showed a more than 10σ deviation to the adopted Atomic Mass Evaluation (AME) value. The reliability of the SHIPTRAP measurement was challenged because the AME value was based on numerous experiments including β and electron capture decays and very precise (n, γ) data, all agreeing with each other. To solve the discrepancy, the $Q_{\text{ee}}(^{102}\text{Pd})$ has now been determined with the JYFLTRAP Penning trap at the IGISOL facility in the Accelerator Laboratory of the University of Jyväskylä. The measurement was performed both with the Time-of-Flight and the Phase-Imaging Ion Cyclotron Resonance techniques. The obtained result, $Q_{\text{ee}}(^{102}\text{Pd}) = 1203.472(45)$ keV, is eight times more precise and agrees well with the value obtained at SHIPTRAP, $Q_{\text{ee}}(^{102}\text{Pd}) = 1203.27(36)$ keV, confirming that ^{102}Pd is not a good candidate for a search for neutrinoless double-electron capture.

Keywords: Penning trap, High-precision mass spectrometry, Q -values, Neutrinoless double-electron capture

1. Introduction

Penning Trap Mass Spectrometry (PTMS) offers versatile opportunities to study fundamental properties of matter via high-precision atomic mass measurements [1]. The method has several advantages:

- Highest precision due to the use of frequency as a measure;
- Sensitivity with the ability to measure the cyclotron frequency for an individual ion;
- Reliability provided by the possibility to use carbon-cluster ions for a direct calibration.

PTMS has been used for investigating fundamental properties in nature, such as Charge Parity Time (CPT) reversal symmetry [1], some problems of quantum chromodynamics (QCD) [2], quantum electrodynamics (QED) [3], and neutrino physics [4]. Values for some fundamental constants in physics can also be explored using PTMS [1]. These experiments require highest achievable precisions. Currently, the record precisions obtained with PTMS are around 10^{-11} [5]. Meanwhile, for many problems in nuclear structure and astrophysics, a few keV precision in nuclear mass values (a relative uncertainty of $\approx 10^{-8}$) is

quite sufficient. However, even with the lower requirements for the precision, the reliability and sensitivity of PTMS remain very important for these measurements.

During the last decade PTMS has shown quite significant discrepancies in the mass differences of certain isobaric nuclides (see e.g. [6, 7, 8]) when compared to the atomic mass evaluations (AME) [9, 10, 11]. In [7], the double electron-capture mass difference Q_{ee} between ^{102}Pd and ^{102}Ru determined at the SHIPTRAP Penning trap, was found to deviate by more than 10 standard deviations from the value given in AME2003 [9]. The case was carefully examined in the next atomic mass evaluation AME2012 [10]. It was found that all data from the flow of information matrix containing various spectroscopic connections are self-consistent and can hardly be erroneous (see Fig. [1]). Thus, the reliability of the PTMS result [7] was seriously questioned. In AME2016 [11], the claim was mitigated by referring to an unpublished less accurate work from the GSI storage ring. However, many arguments given in [10] to support the indirect methods, and thus against the PTMS result, are still valid.

In this work, we have performed a PTMS measurement for the $^{102}\text{Pd} - ^{102}\text{Ru}$ mass difference using the JYFLTRAP Penning trap mass spectrometer. As it is independent of the previous PTMS measurement at SHIPTRAP [7], it provides a way to test the reliability of the method and solve the discrepancy to the other values in the atomic mass evaluations.

*Corresponding author

Email address: dmitrii.nesterenko@jyu.fi (D.A. Nesterenko)

2. Discrepancies in the values for the $^{102}\text{Pd} - ^{102}\text{Ru}$ mass difference

The mass difference of $^{102}\text{Pd} - ^{102}\text{Ru}$ has been previously measured with the SHIPTRAP Penning trap during a campaign searching for a resonant enhancement of neutrinoless double-electron capture. The decay energy (i.e. the mass difference) $Q_{\epsilon\epsilon}(^{102}\text{Pd}) = 1203.27(36)$ keV was determined using the Time-of-Flight Ion Cyclotron Resonance technique [7]. The measured value was 30 keV higher than evaluated in the Atomic Mass Evaluation 2003 (AME2003) [9], $Q_{\epsilon\epsilon}(^{102}\text{Pd}) = 1173.0(24)$ keV. The observed difference of more than 10 standard deviations triggered a thorough analysis on the possible reasons for the discrepancy in AME2012 [10]. Around dozen Q -values were measured using the same procedure in the neutrinoless double-electron capture campaign at SHIPTRAP, and $^{102}\text{Pd} - ^{102}\text{Ru}$ was one of the few cases deviating significantly from AME.

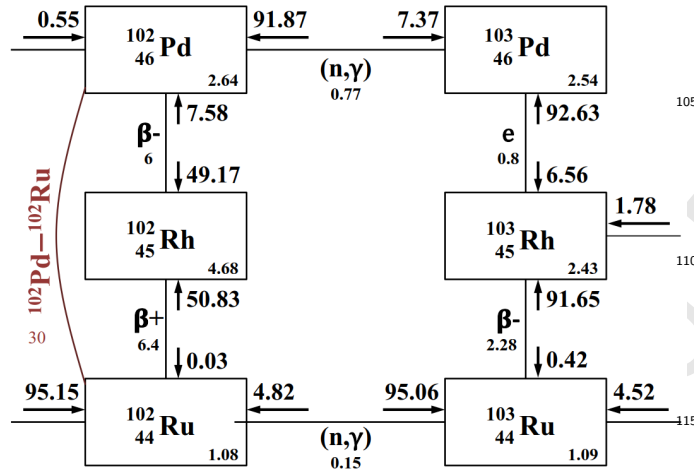


Figure 1: Flow of information diagram [10] showing the connections between ^{102}Pd and ^{102}Ru . The type of relation and its precision (in keV) is given for each connection. The arrows indicate the contribution of the relation in %. The resulting mass precision is given in keV in the lower right corner of each box.

The $Q_{\epsilon\epsilon}$ -value for ^{102}Pd in AME2012 [10] is based on experimental data connecting ^{102}Pd and ^{102}Ru , see Fig. 1. All the measured beta-decay and electron-capture Q -values were collected, and the connections with higher-mass isotopes through precise (n, γ) measurements were taken into account as well. As shown in [10], the $Q_{\epsilon\epsilon}$ -values obtained with these different experimental links agree with each other. Actually all connections have been determined by more than two groups and sometimes with different methods which yield results in good agreement. Thus, it was concluded in [10] that there is no reason to suspect any individual spectroscopic measurement.

From the PTMS side, the result for the mass difference $^{102}\text{Pd} - ^{102}\text{Ru}$ is unlikely to be incorrect. It was measured at SHIPTRAP during the same experimental campaign as $^{106}\text{Cd} - ^{106}\text{Pd}$ and $^{144}\text{Sm} - ^{144}\text{Nd}$ whose PTMS results

are in agreement with the AME values. This makes the case $^{102}\text{Pd} - ^{102}\text{Ru}$ special and calls for a new independent PTMS measurement.

3. Experimental method and results

In this work, the mass difference of ^{102}Pd and ^{102}Ru has been measured with the JYFLTRAP double Penning trap mass spectrometer [12] at the Ion Guide Isotope Separator On-Line (IGISOL) facility [13]. The $^{102}\text{Pd}^+$ and $^{102}\text{Ru}^+$ ions were produced using two different electric discharge ion sources at separate 30 kV high-voltage platforms (see Fig. 2). A natural palladium source was located upstairs in a dedicated offline ion source station whereas the ruthenium ions were produced with a source located inside the IGISOL target chamber. Ions from one ion source at a time were selected by switching voltages on an electrostatic deflector blocking either the vertical (offline station) or horizontal (IGISOL) beamline. A 55° dipole magnet was used to select the $^{102}\text{Pd}^+$ (1.02 % isotopic abundance) and $^{102}\text{Ru}^+$ (31.55 % isotopic abundance) ions from the natural isotopic mixture based on their mass-to-charge ratio of $A/q = 102$. Then, $^{102}\text{Pd}^+$ or $^{102}\text{Ru}^+$ ions were injected into a gas-filled radio-frequency quadrupole [14], where they were cooled and bunched.

The ion bunches were transported to the JYFLTRAP double Penning trap [12] placed inside a 7-T superconducting solenoid. The first preparation trap cooled, centered and additionally purified the ion sample via a mass-selective buffer gas cooling technique [15]. This took around 270 ms for the $^{102}\text{Pd}^+$ and $^{102}\text{Ru}^+$ ions.

The ions from the preparation trap were transferred into the second trap known as the measurement trap where ions' cyclotron frequencies were measured. The traps were operated simultaneously. While the cyclotron frequency of the ions was being measured in the measurement trap, a new bunch of ions was being prepared in the preparation trap.

The cyclotron frequency ν_c of an ion with mass m and charge q in a magnetic field with strength B is given by

$$\nu_c = \frac{1}{2\pi} \frac{q}{m} B. \quad (1)$$

The mass difference between $^{102}\text{Pd}^+$ or $^{102}\text{Ru}^+$ ions was determined from the measured cyclotron frequency ratio R :

$$R = \frac{\nu_c(^{102}\text{Ru}^+)}{\nu_c(^{102}\text{Pd}^+)} = \frac{m(^{102}\text{Pd}^+)}{m(^{102}\text{Ru}^+)} \quad (2)$$

Two different methods were used to measure the cyclotron frequencies ν_c and determine the cyclotron frequency ratio $R = \nu_c(^{102}\text{Ru}^+)/\nu_c(^{102}\text{Pd}^+)$. Firstly, a conventional Time-of-Flight Ion Cyclotron Resonance (ToF-ICR) technique [16, 17] with a 25-750-25 ms (On-Off-On) Ramsey-type excitation pattern [18, 19, 20] was employed (see Fig. 3). For comparison, the SHIPTRAP result of

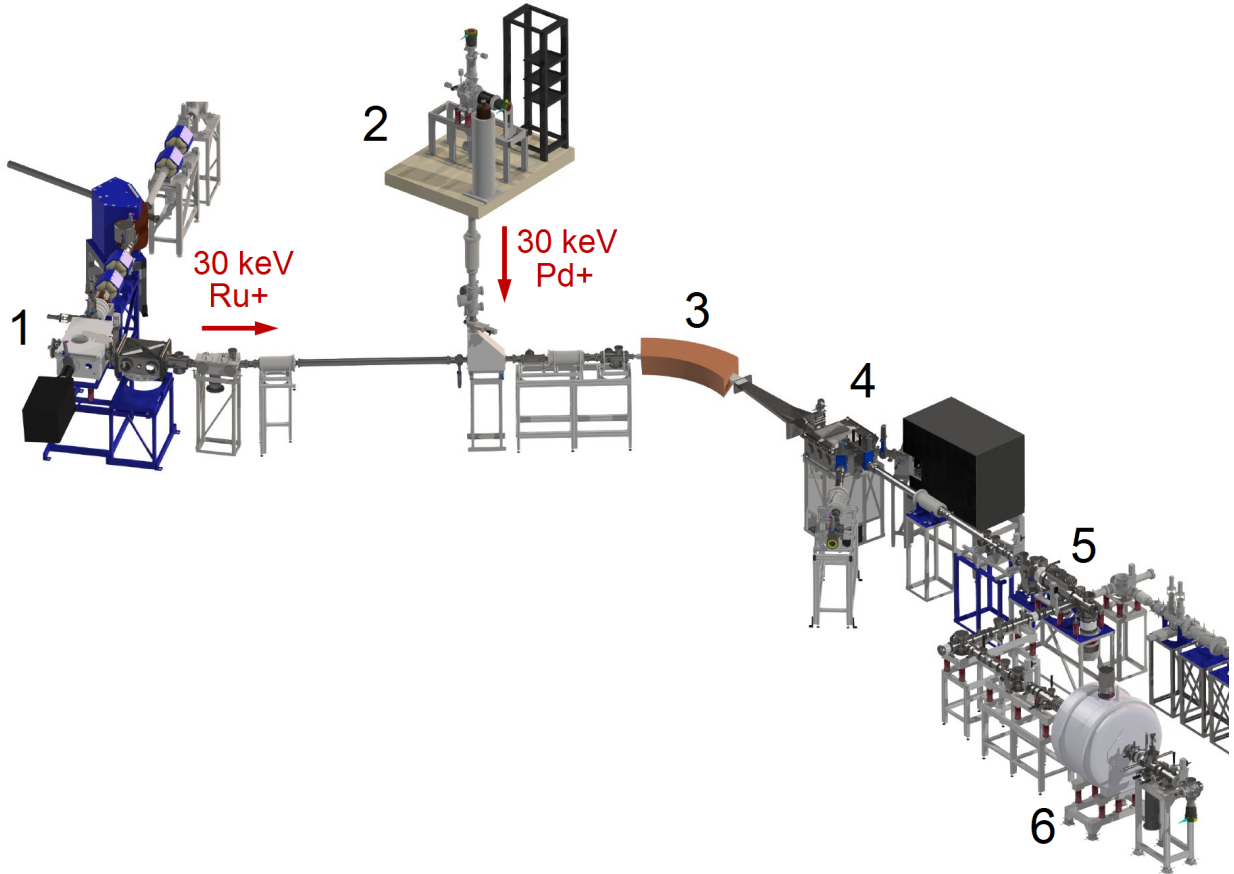


Figure 2: The experimental area of the IGISOL facility, where 1 - the target chamber, 2 - the offline ion source station, 3 - the 55° dipole magnet, 4 - the electrostatic beam switchyard, 5 - the gas-filled radio-frequency quadrupole, 6 - the JYFLTRAP Penning-trap setup.

$Q_{e\epsilon}$ (^{102}Pd)-value [7] was obtained with the ToF-ICR technique and Ramsey-excitation pattern 100-1800-100 ms (On-Off-On). 130

In addition to the ToF-ICR method, we applied the Phase-Imaging Ion Cyclotron Resonance (PI-ICR) technique [21, 22] which has recently been implemented at JYFLTRAP [23]. Here, the cyclotron frequencies for $^{102}\text{Ru}^+$ and $^{102}\text{Pd}^+$ were measured as a sum of two radial-motion 135 frequencies: magnetron frequency ν_- and modified cyclotron frequency ν_+ (the measurement scheme #2 in Ref. [22]). This method has been used in a number of experiments on high-precision Q -value measurements, for example in [3, 24, 25]. 140

The used PI-ICR measurement scheme is shown in Fig. 4. The basic principle of the measurement is to determine the “magnetron” and “cyclotron” phases of ion radial motion on the detector with the positions defined by the polar angles α_- and α_+ , respectively, with respect 145 to the trap center. The angle between the two phase images $\alpha_c = \alpha_+ - \alpha_-$ is related to the cyclotron frequency ν_c by the equation:

$$\nu_c = \nu_- + \nu_+ = (\alpha_c + 2\pi n)/2\pi t, \quad (3) \quad 155$$

where n is the full number of revolutions, which the studied ions would perform in a pure magnetic field B during a

phase accumulation time t . Two different phase accumulation times, 200 ms and 400 ms, were employed for the measurements.

Two excitation patterns were applied to measure the accumulated phases of ion motion and to determine the cyclotron frequency ν_c (see Fig. 4). They differ only by a position of the quadrupolar rf pulse. First, the ions were transported from the preparation trap to the center of the measurement trap and the coherent components of ion’s magnetron and axial motions were reduced via dipolar rf pulses at the corresponding motion frequencies. Then, a dipolar 1-ms rf pulse at modified cyclotron frequency ν_+ was applied to excite the cyclotron motion of ions to a certain radius.

In pattern 1, the cyclotron motion of ions was first converted into the magnetron motion via a quadrupolar 2-ms rf pulse at the cyclotron frequency. Then the ions were let to undergo magnetron motion with the magnetron frequency ν_- for a time t , and accumulate a magnetron-motion phase. After this, ions were extracted out from the measurement trap and their radial positions in the trap were projected onto a position-sensitive detector (a multichannelplate detector with a delay line anode). Thus, pattern 1 provided the image of the magnetron-motion phase of ions with the polar angle α_- (see Fig. 5).

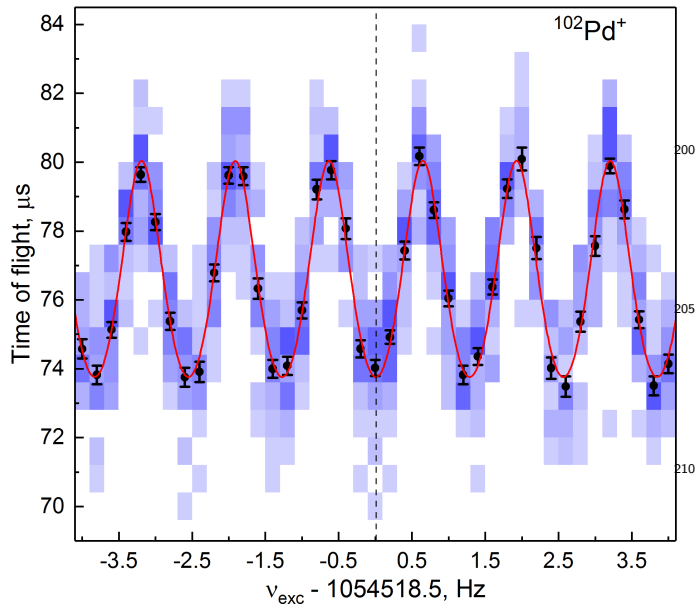


Figure 3: A typical time-of-flight resonance of $^{102}\text{Pd}^+$ with 25-750-25 ms (On-Off-On) Ramsey excitation pattern. The black points with error bars represent the mean time-of-flight for each scanned frequency. The solid red line is a fit of the theoretical curve [20] to the data points. The blue shading around the data points indicates the number of ions in each time-of-flight bin: the darker the blue, the more ions. The position of the central minimum was determined before the measurements using conventional ToF-ICR with a single 800-ms excitation pulse [17].

In pattern 2, the ions performed the cyclotron motion for a time t , accumulating a cyclotron-motion phase. Before extracting the ions out from the measurement trap, a quadrupolar 2-ms rf pulse at the cyclotron frequency was applied in order to convert the fast cyclotron motion to the slow magnetron motion. The positions of the extracted ions were projected onto a position-sensitive detector similarly to pattern 1. Pattern 2 provided the image of the cyclotron-motion phase of ions with the polar angle α_+ (see Fig. 5). Note that the complete conversion of the cyclotron motion to the magnetron motion preserves the modulus of the angle for the accumulated phase although flipping the sign of the angle [22, 26].

The patterns 1 and 2 were applied alternately to obtain the images of magnetron and cyclotron phases (see Fig. 5). Thus, determination of the angles α_- and α_{+240} were performed quasi-simultaneously. The trap center on the detector was determined once per around 3.5 hours, i.e. before and after each measurement set. To reduce possible distortions in the ion-motion projections onto the detector, the positions of the magnetron and cyclotron phase images were chosen such that the angle α_c did not exceed a few degrees. To average the ion positions over all magnetron phases and eliminate the possible angular shift of the centroid position due to possible residual magnetron motion (after its coherent component had been reduced), the start time of the dipolar excitation pulse at the frequency ν_+ was scanned over a magnetron period ($\approx 600 \mu\text{s}$). In ad-

dition, the start time of the extraction pulse was scanned over a cyclotron period ($\approx 0.95 \mu\text{s}$) to average the ion positions over all cyclotron phases in order to eliminate possible residual cyclotron motion after the conversion. Note that the ion interactions with the residual gas molecules in the measurement trap decrease the radius of the fast cyclotron motion and smear the image of the cyclotron phase spot [22], increasing the statistical uncertainty but not causing a systematic shift.

The cyclotron frequency measurements for $^{102}\text{Ru}^+$ and $^{102}\text{Pd}^+$ were performed alternately for several days. For ToF-ICR, the ions were swapped after each frequency scan (≈ 1.3 min). For PI-ICR, two measurement rounds with $t_{acc} = 400$ ms (around ≈ 47 s), or three rounds with $t_{acc} = 200$ ms (≈ 41 s), were carried out before swapping between the $^{102}\text{Ru}^+$ and $^{102}\text{Pd}^+$ ions.

The data for $^{102}\text{Ru}^+$ and $^{102}\text{Pd}^+$ were grouped in the data analysis by 10, 8 and 9 rounds for ToF-ICR, PI-ICR with $t_{acc} = 400$ ms and PI-ICR with $t_{acc} = 200$ ms measurements, respectively, to obtain enough statistics for fitting (600-900 ions). The cyclotron frequency of $^{102}\text{Ru}^+$, measured before and after $^{102}\text{Pd}^+$, was linearly interpolated to the measurement time of $^{102}\text{Pd}^+$ to determine a single frequency ratio. Altogether 15 around 3.5-hour measurement periods were performed. For each period, a weighted mean of the frequency ratio $R_{3.5h}$ was calculated. The maximum of the internal and external errors has been chosen for the weighted mean frequency ratios $R_{3.5h}$.

The nonlinear drift of the magnetic field between two neighboring frequency measurements was negligible compared to the statistical errors. The mass-dependent uncertainties were neglected because $^{102}\text{Pd}^+$ - $^{102}\text{Ru}^+$ is a mass doublet with the same A/q . Count-rate class analysis [27] was performed for the determined cyclotron frequency ratios to study ion-ion interactions. The data were divided into five groups according to the number of detected ions per bunch. No dependence of the frequency ratio on the number of detected ions were observed (see Fig. 6), and only data up to 5 ions/bunch were taken into account in the analysis. For the PI-ICR technique, the systematic errors due to non-simultaneous measurements of the center and the phase positions, and the distortion of the ion-motion projection onto the detector, were around 50-70% of the statistical errors.

Figure 7 shows the frequency ratios $R_{3.5h}$ measured in this work. The first six measurements were performed with the ToF-ICR technique and the subsequent nine with the PI-ICR technique. The uncertainties of $R_{3.5h}$ are similar in both methods because the excitation time in the ToF-ICR technique was four times longer than the phase accumulation time in the PI-ICR technique, and additional systematic errors were added for the PI-ICR measurements. The calculated Birge ratio [28] was 0.98 supporting that all systematic uncertainties have been properly taken into account. The higher, internal uncertainty, was adopted for the final weighted mean of cyclotron ratios $R_{3.5h}$, $\bar{R} = 1.00001267844(47)$.

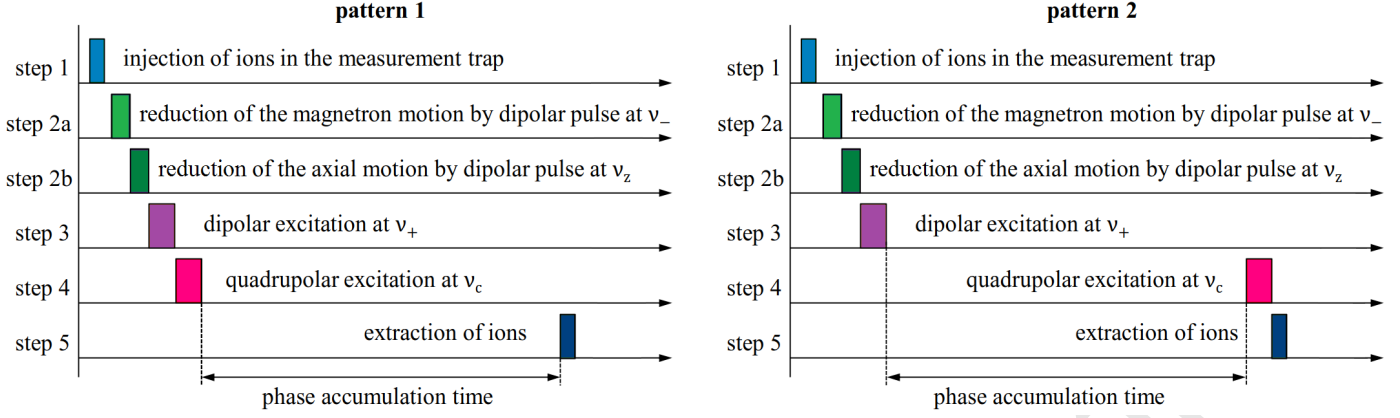


Figure 4: Measurement pulse scheme for the cyclotron frequency determination ν_c in the PI-ICR technique. The magnetron and cyclotron phases are accumulated in the patterns 1 and 2, respectively.

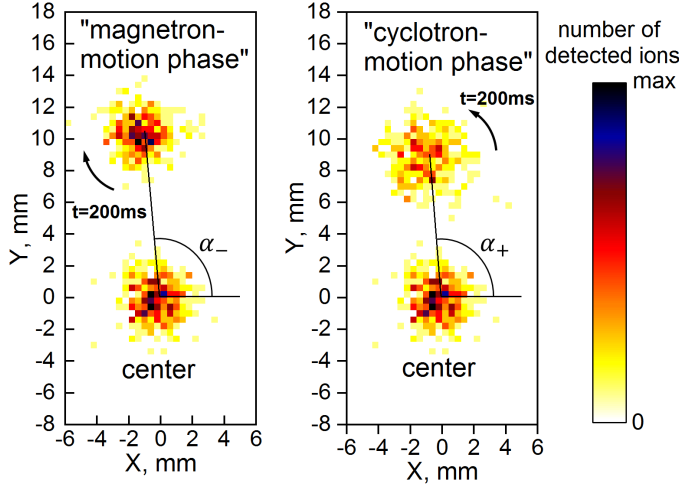


Figure 5: The trap center and accumulated phase spots for $^{102}\text{Pd}^+$ ions on the position-sensitive ion detector for a single cyclotron frequency measurement (≈ 2 min) with the phase accumulation time $t_{acc} = 200$ ms. The magnetron-motion phase was accumulated using pattern 1 and the cyclotron-motion phase with pattern 2 of the excitation-pulse scheme.

The $Q_{e\epsilon}$ -value can be calculated from the cyclotron frequency ratio as

$$Q_{e\epsilon} = m(^{102}\text{Pd}) - m(^{102}\text{Ru}) = (m(^{102}\text{Ru}) - m_e)(R - 1), \quad (4)$$

where $m(^{102}\text{Pd})$ and $m(^{102}\text{Ru})$ are atomic masses of ^{102}Pd and ^{102}Ru , respectively, m_e is the electron mass and R is the cyclotron frequency ratio of singly charged ions of ^{102}Ru and ^{102}Pd , respectively. The difference of binding energies of the valence electrons for ^{102}Ru and ^{102}Pd is less than 2.5 eV [29], and can be neglected.

Thus, the final cyclotron frequency ratio \bar{R} results in $Q_{e\epsilon} = 1203.472(45)$ keV. It is in a good agreement with the value obtained at SHIPTRAP [7], $Q_{e\epsilon} = 1203.27(36)$ keV, and is eight times more precise.

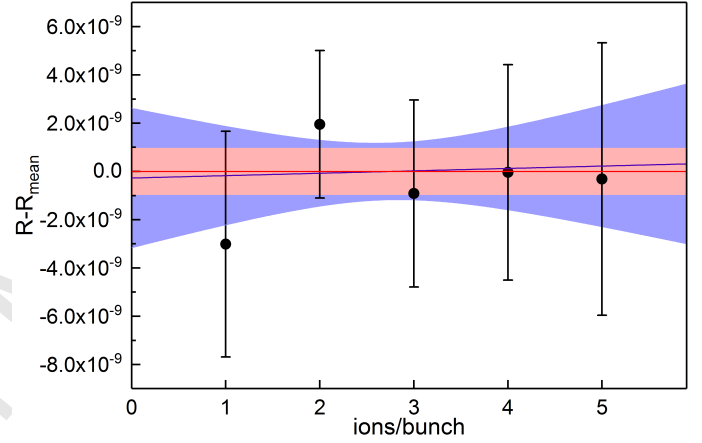


Figure 6: The cyclotron frequency ratio as a function of the number of detected ions per bunch for one of the 3.5-hour measurement periods. The blue line marks a linear fit. The 1σ confidence band of the fit is shown in blue. The red line and the red-shaded band mark the mean of the ratio, averaged over one to five ions per bunch, and the 1σ uncertainty, respectively. The slope of the linear fit is in agreement with the mean value within the confidence band for all measurement periods.

4. Conclusions

The new precise direct measurement of the mass difference $^{102}\text{Pd} - ^{102}\text{Ru}$ with the JYFLTRAP Penning trap mass spectrometer is in a good agreement with the previous Penning-trap measurement performed at SHIPTRAP. Therefore, it confirms that the SHIPTRAP PTMS result is correct and calls for a reanalysis of mass and spectroscopic data that lead to a more than 10σ deviation to the adopted mass evaluation value. It is worthwhile to note that in AME2016, two pieces of data, $^{102}\text{Rh}(\beta^-)^{102}\text{Pd}$ and $^{103}\text{Pd}(EC)^{103}\text{Rh}$, have already been discarded. Our result also confirms the conclusion from the SHIPTRAP measurement [7] that there is no resonant enhancement for search for neutrinoless double-electron capture in ^{102}Pd . In conclusion, Penning-trap mass spectrometry is a reliable and precise method to determine atomic masses for

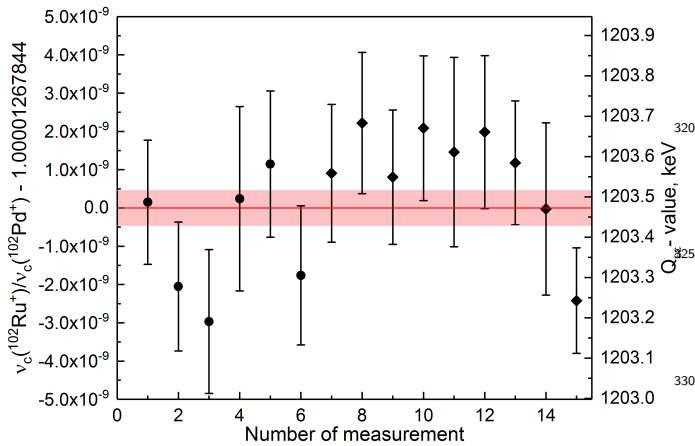


Figure 7: The measured cyclotron frequency ratios $\nu_c(^{102}\text{Ru}+)/\nu_c(^{102}\text{Pd}+) - 1.00001267844$ (the axis on the left) and Q_{ec} values (the axis on the right) determined in this work. Each point represents one around 3.5-hour measurement. The red-shaded band shows the total uncertainty of the weighted mean.

fundamental physics problems, neutrino physics, nuclear physics as well as for astrophysics.

Acknowledgements

This work has been supported by the Academy of Finland by the project "State-of-the-art ion beam developments for JYFL-ACCLAB", decision No. 273526. A.K. acknowledges the support from the Academy of Finland under grant No. 275389 and D.N. and L.C. under grants No. 284516 and 312544. T.E. acknowledges the support from the Academy of Finland under grant No. 295207 and A.R. under grant No. 306980.

References

- [1] K. Blaum, Y. N. Novikov, G. Werth, Penning traps as a versatile tool for precise experiments in fundamental physics, *Contemporary Physics* 51 (2) (2010) 149–175. [doi:10.1080/00107510903387652](https://doi.org/10.1080/00107510903387652).
- [2] T. Eronen, J. C. Hardy, High-precision Q_{ec} -value measurements for superallowed decays, *Eur. Phys. J. A* 48 (4) (2012) 48.
- [3] F. Köhler, et al., Isotope dependence of the Zeeman effect in lithium-like calcium, *Nature Communications* 7 (2016) 10246. [doi:10.1038/ncomms10246](https://doi.org/10.1038/ncomms10246).
- [4] S. Eliseev, T. Eronen, Y. N. Novikov, Penning-trap mass spectrometry for neutrino physics, *International Journal of Mass Spectrometry* 349-350 (2013) 102 – 106, 100 years of Mass Spectrometry. [doi:doi.org/10.1016/j.ijms.2013.03.010](https://doi.org/10.1016/j.ijms.2013.03.010).
- [5] S. Rainville, et al., A direct test of $E = mc^2$, *Nature* 438 (2005) 1096. [doi:10.1038/4381096a](https://doi.org/10.1038/4381096a).
- [6] S. Eliseev, et al., Direct mass measurements of ^{194}Hg and ^{194}Au : A new route to the neutrino mass determination?, *Physics Letters B* 693 (4) (2010) 426 – 429. [doi:10.1016/j.physletb.2010.08.071](https://doi.org/10.1016/j.physletb.2010.08.071).
- [7] M. Goncharov, K. Blaum, M. Block, C. Droese, S. Eliseev, F. Herfurth, E. Minaya Ramirez, Y. N. Novikov, L. Schweikhard, K. Zuber, Probing the nuclides ^{102}Pd , ^{106}Cd , and ^{144}Sm for resonant neutrinoless double-electron capture, *Phys. Rev. C* 84 (2011) 028501. [doi:10.1103/PhysRevC.84.028501](https://doi.org/10.1103/PhysRevC.84.028501).
- [8] D. A. Nesterenko, et al., Double- β transformations in isobaric triplets with mass numbers $A = 124, 130$, and 136 , *Phys. Rev. C* 86 (2012) 044313. [doi:10.1103/PhysRevC.86.044313](https://doi.org/10.1103/PhysRevC.86.044313).
- [9] G. Audi, O. Bersillon, J. Blachot, A. Wapstra, The Nubase evaluation of nuclear and decay properties, *Nuclear Physics A* 729 (1) (2003) 3 – 128, the 2003 NUBASE and Atomic Mass Evaluations. [doi:https://doi.org/10.1016/j.nuclphysa.2003.11.001](https://doi.org/10.1016/j.nuclphysa.2003.11.001).
- [10] G. Audi, M. Wang, A. Wapstra, F. Kondev, M. MacCormick, X. Xu, B. Pfeiffer, The Amc2012 atomic mass evaluation, *Chinese Physics C* 36 (12) (2012) 1287. URL <http://stacks.iop.org/1674-1137/36/i=12/a=002>.
- [11] W. Huang, G. Audi, M. Wang, F. Kondev, S. Naimi, X. Xu, The AME2016 atomic mass evaluation (i). evaluation of input data; and adjustment procedures, *Chinese Physics C* 41 (3) (2017) 030002. URL <http://stacks.iop.org/1674-1137/41/i=3/a=030002>.
- [12] T. Eronen, et al., JYFLTRAP: a Penning trap for precision mass spectroscopy and isobaric purification, *Eur. Phys. J. A* 48 (4) (2012) 46. [doi:10.1140/epja/i2012-12046-1](https://doi.org/10.1140/epja/i2012-12046-1).
- [13] I. Moore, et al., Towards commissioning the new IGISOL-4 facility, *Nucl. Instrum. Meth. Phys. Res. B* 317 (2013) 208 – 213, XVth International Conference on ElectroMagnetic Isotope Separators and Techniques Related to their Applications, December 27, 2012 at Matsue, Japan. [doi:10.1016/j.nimb.2013.06.036](https://doi.org/10.1016/j.nimb.2013.06.036).
- [14] A. Nieminen, J. Huikari, A. Jokinen, J. Äystö, P. Campbell, E. Cochrane, Beam cooler for low-energy radioactive ions, *Nucl. Instrum. Meth. Phys. Res. A* 469 (2) (2001) 244 – 253. [doi:10.1016/S0168-9002\(00\)00750-6](https://doi.org/10.1016/S0168-9002(00)00750-6).
- [15] G. Savard, S. Becker, G. Bollen, H. J. Kluge, R. B. Moore, T. Otto, L. Schweikhard, H. Stolzenberg, U. Wiess, A new cooling technique for heavy ions in a Penning trap, *Phys. Lett. A* 158 (5) (1991) 247 – 252. [doi:10.1016/0375-9601\(91\)91008-2](https://doi.org/10.1016/0375-9601(91)91008-2).
- [16] G. Gräff, H. Kalinowsky, J. Traut, A direct determination of the proton electron mass ratio, *Z. Phys. A* 297 (1) (1980) 35–39. [doi:10.1007/BF01414243](https://doi.org/10.1007/BF01414243).
- [17] M. König, G. Bollen, H. J. Kluge, T. Otto, J. Szerypo, Quadrupole excitation of stored ion motion at the true cyclotron frequency, *Int. J. Mass Spectrom. Ion Processes* 142 (1-2) (1995) 95 – 116. [doi:10.1016/0168-1176\(95\)04146-C](https://doi.org/10.1016/0168-1176(95)04146-C).
- [18] S. George, et al., Ramsey method of separated oscillatory fields for high-precision Penning trap mass spectrometry, *Phys. Rev. Lett.* 98 (2007) 162501. [doi:10.1103/PhysRevLett.98.162501](https://doi.org/10.1103/PhysRevLett.98.162501).
- [19] S. George, K. Blaum, F. Herfurth, A. Herlert, M. Kretzschmar, S. Nagy, S. Schwarz, L. Schweikhard, C. Yazidjian, The Ramsey method in high-precision mass spectrometry with Penning traps: Experimental results, *Int. J. Mass Spectrom.* 264 (23) (2007) 110 – 121. [doi:10.1016/j.ijms.2007.04.003](https://doi.org/10.1016/j.ijms.2007.04.003).
- [20] M. Kretzschmar, The Ramsey method in high-precision mass spectrometry with Penning traps: Theoretical foundations, *Int. J. Mass Spectrom.* 264 (23) (2007) 122 – 145. [doi:10.1016/j.ijms.2007.04.002](https://doi.org/10.1016/j.ijms.2007.04.002).
- [21] S. Eliseev, K. Blaum, M. Block, C. Droese, M. Goncharov, E. Minaya Ramirez, D. A. Nesterenko, Y. N. Novikov, L. Schweikhard, Phase-imaging ion-cyclotron-resonance measurements for short-lived nuclides, *Phys. Rev. Lett.* 110 (2013) 082501. [doi:10.1103/PhysRevLett.110.082501](https://doi.org/10.1103/PhysRevLett.110.082501).
- [22] S. Eliseev, et al., A phase-imaging technique for cyclotron-frequency measurements, *Applied Physics B* 114 (1) (2014) 107–128. [doi:10.1007/s00340-013-5621-0](https://doi.org/10.1007/s00340-013-5621-0).
- [23] D. A. Nesterenko, et al., Phase-Imaging Ion-Cyclotron-Resonance technique at the JYFLTRAP double Penning trap mass spectrometer, *Eur. Phys. J. A* 54 (2018) 154. [doi:10.1140/epja/i2018-12589-y](https://doi.org/10.1140/epja/i2018-12589-y).
- [24] D. A. Nesterenko, et al., Direct determination of the atomic mass difference of ^{187}Re and ^{187}Os for neutrino physics and cosmochronology, *Phys. Rev. C* 90 (2014) 042501. [doi:10.1103/PhysRevC.90.042501](https://doi.org/10.1103/PhysRevC.90.042501).
- [25] S. Eliseev, et al., Direct measurement of the mass difference of ^{163}Ho and ^{163}Dy solves the Q-value puzzle for the neutrino

- mass determination, Phys. Rev. Lett. 115 (2015) 062501. doi:
[10.1103/PhysRevLett.115.062501](https://doi.org/10.1103/PhysRevLett.115.062501).
- 390 [26] M. Kretzschmar, On the phase dependence of the interconversion of the motional modes in a Penning trap by quadrupolar excitation, Int. J. Mass Spectrom. 309 (2012) 30 – 38. doi:
[10.1016/j.ijms.2011.08.022](https://doi.org/10.1016/j.ijms.2011.08.022).
- 395 [27] C. Roux, K. Blaum, M. Block, C. Droese, S. Eliseev, M. Goncharov, F. Herfurth, E. M. Ramirez, D. A. Nesterenko, Y. N. Novikov, L. Schweikhard, Data analysis of q-value measurements for double-electron capture with shiptrap, The European Physical Journal D 67 (7) (2013) 146. doi:
[10.1140/epjd/e2013-40110-x](https://doi.org/10.1140/epjd/e2013-40110-x).
- 400 [28] R. T. Birge, The calculation of errors by the method of least squares, Phys. Rev. 40 (1932) 207–227. doi:
[10.1103/PhysRev.40.207](https://doi.org/10.1103/PhysRev.40.207).
- [29] F. Larkins, Semiempirical Auger-electron energies for elements $10 \leq Z \leq 100$, Atomic Data and Nuclear Data Tables 20 (4) (1977) 311 – 387. doi:
[10.1016/0092-640X\(77\)90024-9](https://doi.org/10.1016/0092-640X(77)90024-9).

The submitted manuscript describes the measurement of mass difference between ^{102}Pd and ^{102}Ru performed with the Penning-trap mass spectrometer JYFLTRAP. A very careful evaluation on the atomic mass difference of the pair $^{102}\text{Pd} - ^{102}\text{Ru}$ in the Atomic Mass Evaluation based on the analysis of full bulk of spectroscopy information for nearest nuclides showed a dramatic deviation of more than 10σ with the mass measurement performed at the SHIPTRAP Penning trap. Since the evaluated mass difference was obtained via numerous local connections in β - and electron capture decays and very precise (n,γ) data which agree with each other perfectly, the reliability of the SHIPTRAP measurement was challenged. To solve the problem, the measurement of the mass difference $^{102}\text{Pd} - ^{102}\text{Ru}$ has been undertaken at the JYFLTRAP Penning-trap setup using both the Time-of-Flight and the Phase-Imaging Ion Cyclotron Resonance techniques. The obtained result is around 8 times more precise and in excellent agreement with the value obtained at SHIPTRAP. This agreement manifests the reliability of the Penning trap mass spectrometry.